

Beta decay of ^{15}C

D. E. Alburger and D. J. Millener

Brookhaven National Laboratory, Upton, New York 11973

(Received 8 June 1979)

The spectrum of γ rays following the β decay of ^{15}C , produced in the $^{13}\text{C}(t,p)^{15}\text{C}$ reaction, has been studied with a 50-cm³ Ge(Li) detector. Allowed β -ray branches to all available ^{15}N excited states known to have $J^\pi = 1/2^+$ or $3/2^+$ were measured including a branch to the 8571-keV state not reported previously. A value of 2.449 ± 0.005 sec was obtained for the ^{15}C half-life by multiscaling β rays detected in a plastic scintillator. The experimental ^{15}C β -ray transition rates are compared with theoretical calculations.

RADIOACTIVITY ^{15}C ; measured E_γ , I_γ , $t_{1/2}$; deduced decay scheme and experimental $\log ft$ values; calculated $\log ft$ values from theory; compared experiment with theory.

I. INTRODUCTION

^{15}C is known¹ to decay by β -ray emission to ^{15}N with a half-life of 2.45 sec and a total decay energy of 9772 keV. Principal β -ray branches lead to the 5299-keV $\frac{1}{2}^+$ second-excited state of ^{15}N (68%) and to the $\frac{1}{2}^-$ ground state (32%). These branches, as well as evidence that ^{15}C has a spin-parity $J^\pi = \frac{1}{2}^+$, were established some years ago.^{2,3} Above an excitation energy of 5299 keV in ^{15}N there are four states, namely those at 7301, 8313, 8571, and 9050 keV, which have¹ spin-parities of $\frac{1}{2}^+$ or $\frac{3}{2}^+$ and which should be populated by allowed β -ray branches from ^{15}C . Early theoretical calculations² indicated the expected β transition rates to some of these states.

Past experimental efforts in finding the four additional expected ^{15}C β -decay branches have met with only partial success.^{4,5} In all previous experiments the ^{15}C activity was produced in the $^{14}\text{C}(d,p)^{15}\text{C}$ reaction and evidence for the β -ray branches consisted of observing the subsequent high-energy γ -ray decays of the states in a Ge(Li) detector. All of these states are known to decay predominantly by ground-state γ -ray transitions. Because of the severe radioactivity contamination problem associated with ^{14}C targets it was necessary to use a fixed target-detector geometry and to chop the beam for an irradiate-count sequence. Several difficulties in establishing these β -ray branches included the weakness of the transitions, the low efficiency of the detectors for high-energy γ rays, and the relatively high background due to bremsstrahlung radiation. Even with the best resolution and highest efficiency Ge(Li) detectors it was difficult to observe the full-energy or annihilation escape peaks above background. Longer runs could have been made to improve the statistical accuracy, but there was the additional problem of radiation damage to the

Ge(Li) detector due to neutrons from the $^{14}\text{C}(d,n)$ and $^{12}\text{C}(d,n)$ reactions. Shifting of the peaks and degradation of the energy resolution occurred before sufficient statistical accuracy could be obtained.

The return to the ^{15}C problem as reported here was brought about by two technical improvements to the 3.5-MV Van de Graaff facility at this laboratory. One of these was the installation some years ago of a triton beam system which permits the production of ^{15}C via the $^{13}\text{C}(t,p)^{15}\text{C}$ reaction and another was the construction of a "rabbit" target-transfer system. Thus the ^{13}C targets could be irradiated and transported, without the previous contamination problem, to a remote Ge(Li) detector that was free from neutron exposure and therefore stable in its gain and resolution characteristics over long counting periods. All four of the expected weak β -ray branches are now established and we further report a new value for the ^{15}C half-life.

There have been rather few theoretical calculations of the β -decay scheme of ^{15}C . The theoretical $\log ft$ values quoted in the latest tabulation¹ were computed² using the wave functions of Halbert and French⁶ which are over twenty years old. However, there have in fact been at least three subsequent attempts⁷⁻⁹ to describe the β transitions to the positive parity levels of ^{15}N . In addition, Towner and Hardy¹⁰ have performed calculations for the first-forbidden nonunique decay of ^{15}C to the ground state of ^{15}N .

Since the calculation of Halbert and French, which used the full space of $1\hbar\omega$ configurations with spurious center-of-mass states eliminated, there have been numerous shell-model calculations for the positive parity levels of the $A = 15$ nuclei. The calculations of Zhusupov, Karapetyan, and Eramzhan⁷ and Hsieh and Horie⁸ are similar to those of Halbert and French. More recently, still within

the framework of a $1\hbar\omega$ model space, Hsieh *et al.*¹¹ have used a particle-hole interaction obtained by varying selected matrix elements to fit the " $1\hbar\omega$ spectra" of $A=15, 16$, and 17 . One of the most comprehensive and physically appealing calculations to date is the weak-coupling calculation by Lie, Engeland, and Dahll¹² which includes $3p$ - $4h$ configurations in the model space. The lowest $3p$ - $4h$ states are expected to occur quite low in energy¹²⁻¹⁴ and indeed are necessary to give the correct number of $\frac{1}{2}^+$, $\frac{3}{2}^+$, and $\frac{5}{2}^+$ levels below ~ 10 MeV in excitation energy. Other calculations¹⁵⁻¹⁷ have started with a $s_{1/2}^4 p_{3/2}^8$ core and used a restricted $p_{1/2} s_{1/2} d_{5/2}$ model space.

In most of the above calculations, the full $1\hbar\omega$ calculations excepted, the choice of model space precludes a complete separation of spurious center-of-mass states. In some calculations the problem has simply been ignored, and for some spaces this may be the best approach,¹⁸ while in others, e.g., Ref. 12, largely spurious states have been projected out of the basis and eliminated. The calculations based on a $s_{1/2}^4 p_{3/2}^8$ core are of limited value for a discussion of the ^{15}C β -decay since the omission of one member of a spin-orbit doublet is an unreliable procedure when calculating the matrix elements of spin-dependent operators (see Sec. IV A).

In Sec. IV we present a general discussion of the positive parity levels of ^{15}N as it pertains to the β decay of ^{15}C . Calculations are described which include all $1\hbar\omega$ and some $3\hbar\omega$ configurations. These calculations may be most directly compared with those of Lie, Engeland, and Dahll.¹² The calculated $\log ft$ values are presented and compared with the experimental data and previous calculations. We attempt to show that the $\log ft$ values for the $\frac{1}{2}^+ \rightarrow \frac{1}{2}^+$ transitions in particular represent a stringent test for the model wave functions.

II. EXPERIMENTAL METHODS

The ^{15}C activity was produced in a self-supporting carbon foil ~ 10 mg/cm² thick and enriched to 90% in ^{13}C , by the $^{13}\text{C}(t,p)^{15}\text{C}$ reaction using 3.0-MeV tritons from the 3.5-MV Van de Graaff. The foil was clamped in a "rabbit" for transport from the bombardment position through a shielding wall to the detector located in the accelerator control room. For the γ -ray measurements a 50-cm³ Ge(Li) detector was separated from the rabbit line by a 1.3-cm thick graphite slab to absorb β rays with low bremsstrahlung production. The output of the detector was fed to a linear amplifier and thence to an 8192-channel pulse-height analyzer.

The operation of the rabbit system and data stor-

age was controlled automatically by a timer-programmer.¹⁹ After an irradiation of the target with a 3.0-MeV triton beam of ~ 40 nA for 1.5 sec, the sample was transferred in 0.7 sec to the detector and counted for 3 sec by gating on the analyzer. The actual beam current was adjusted so that the initial total counting rate was 6000-7000 per sec so as to result in optimum statistical accuracy without degrading the detector resolution. At the end of the count the rabbit was returned in 0.6 sec for another irradiation.

Another function carried out by the timer-programmer was to extinguish the Van de Graaff rf ion source thereby completely removing the beam during the rabbit-transfer and counting periods. This was done by operating a solenoid-string-micro switch system inside the terminal of the Van de Graaff which disconnected the plate voltage from the rf oscillator. There was no delay in resumption of the source operation upon reconnecting the voltage. While the source was off the voltage regulation of the Van de Graaff terminal, normally accomplished by a slit feedback system sensing the fringes of the two sides of the beam, automatically transferred to control by a null-reading generating voltmeter. Reappearance of the beam caused the regulation to switch back to the slits. This system, rather than a pneumatically operated beam interceptor, was adopted in order to remove completely the machine background of neutrons and high-energy γ rays. When a beam interceptor was tried the general background was higher and the 7.6-MeV γ -ray doublet from the $^{56}\text{Fe}(n,\gamma)^{57}\text{Fe}$ reaction could be detected in the spectrum even though the Ge(Li) detector was located in the control room.

For the half-life measurements on ^{15}C an NE102 plastic scintillator 5 cm in diameter by 2.5 cm thick mounted on a photomultiplier tube was placed close to a Be window in the transfer line where the irradiated rabbit sample stopped. Pb shielding was used to reduce the room background. The techniques for multiscaling the β rays were similar to those described previously.²⁰

III. EXPERIMENTAL RESULTS AND ANALYSIS

A. γ -ray spectrum

The γ -ray spectrum of ^{15}C was recorded for a total of approximately 100 hours in successive runs of ~ 20 h each. After each individual run the data were taped and the analyzer cleared so that the spectrum of each run could be plotted on the computer to inspect the positions of various peaks. A very small gain shift (~ 1 channel at ~ 7 MeV) occurred after the first 50 hours. The data of the two halves of the run were matched in gain and

then added.

Each of the weak peaks in the final spectrum was analyzed with a computer program which fitted the data in the vicinity of a peak with a Gaussian plus a linear or quadratic background. The position, full-width-at-half-maximum (FWHM), and net area of the peak, and the constants of the background function could be treated as variables or fixed. The procedure adopted was to find the FWHM's of the strongest peaks including those due to the 6129- and 7115-keV γ rays of ^{16}N which were present in the spectra and presumably were produced by the $^{14}\text{N}(t, p)^{16}\text{N}$ reaction on contaminant nitrogen in the target. A plot was then made of FWHM versus energy which was an approximately linear function from 5.3 to 9 MeV and was so assumed. This procedure was used to fix the FWHM expected for any weak peak at a given point in the spectrum. The program then found the peak position and its net area, the FWHM having been specified.

An example of the data and analysis is given in Fig. 1 which shows the γ -ray spectrum of ^{15}C in the vicinity of the 9047(2) and 8569(1) peaks. [throughout this paper (0), (1), and (2) indicate full energy loss, one-escape, and two-escape

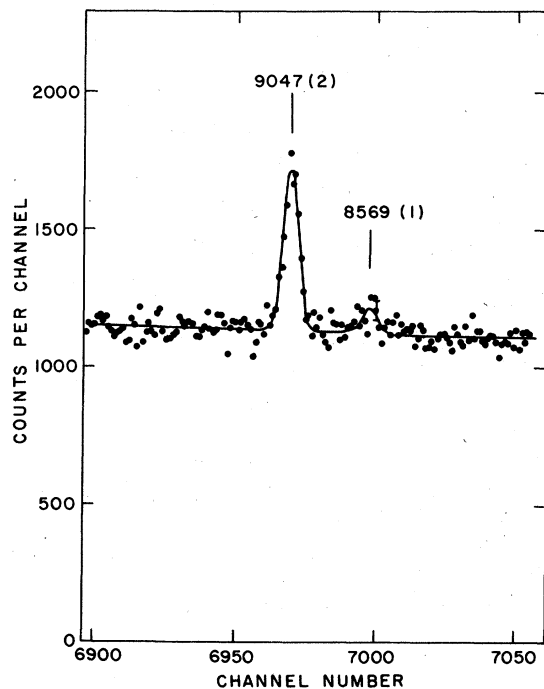


FIG. 1. γ -ray spectrum of ^{15}C in the region of the 9047(2) and 8569(1) lines obtained in a run of 100 h duration. As explained in the text the solid line is a computer fit which gives 4005 ± 133 and 549 ± 113 net counts, respectively, for the two peaks.

peaks, respectively.] Of all of the γ rays the one at 8569 keV was the weakest and most difficult one to detect. In Fig. 1 the two peaks were each analyzed with zero weighting of all points in the other peak and the solid line is the overall computer fit. Thus the program found an area of 549 ± 113 net counts in the 8569(1) peak and established its position with an accuracy of ± 0.76 channels (± 0.87 keV). On the other hand the 9047(2) peak had a net area of 4005 ± 133 counts and the error in its peak position was ± 0.12 channels (± 0.14 keV). In other regions of the spectrum, not shown, the 8569(2) peak was found to have a net area of 600 ± 98 counts and the 8569(0) peak had a net area of 316 ± 98 counts. Not only did the positions of these three peaks all correspond to the same γ -ray energy to within ± 0.7 keV, but their relative areas agreed within errors with the known ratios of (0), (1), and (2) peak intensities versus γ -ray energy for the detector used. Thus the presence of the 8569-keV γ ray was firmly established.

The γ ray at 7299 keV produced one- and two-escape peaks with areas of 1116 ± 116 and 1123 ± 116 net counts, respectively. The full-energy peak of this transition was also observed, but it was too close to the 8311(2) peak for a reliable intensity determination.

In order to obtain the relative peak efficiency function versus γ -ray energy, the Ge(Li) detector was moved to the high-flux reactor and the spectrum from the $^{53}\text{Cr}(n, \gamma)^{54}\text{Cr}$ reaction was recorded using the same geometry and absorbers as in the ^{15}C runs. Relative intensities of the Cr γ rays have been listed²¹ by Kane and Mariscotti. Using the measured γ rays between 3.7 and 8.9 MeV, curves of efficiency versus energy were developed for the full-energy, one-escape, and two-escape peaks. For the one- and two-escape peaks the efficiency between 5.3 and 9 MeV decreased by only about 30%, whereas the full-energy peak efficiency decreased by a factor of 3 over the same range. At a γ -ray energy of about 5.7 MeV all three peak efficiencies were nearly the same. Since the Cr γ -ray relative intensities are accurate to about $\pm 6\%$, a generous error of $\pm 8\%$ was adopted for the efficiency when comparing high-energy γ rays of ^{15}C to the 5.3-MeV γ ray.

The final value for the relative intensity of each γ ray was determined from the weighted average of the results based on the separate peak areas each corrected by the corresponding efficiency curve. Since the peaks due to the 5298-keV γ ray spilled over many times during each run due to the limit in analyzer storage capacity of 99 999 counts per channel their total areas for the complete run were determined by measuring the peak

TABLE I. γ -ray energies and relative intensities measured in the decay of ^{15}C . Present and previous ^{15}N excitation energies are listed.

E_γ (keV) Present	E_{exc} in ^{15}N (keV)		I_γ (% per decay) present
	Present	Previous ^a	
5297.86 \pm 0.15 ^b	5298.87 \pm 0.15 ^b	5299.16 \pm 0.12	68 \pm 2 ^c
6321.9 \pm 0.6	6323.3 \pm 0.6	6323.85 \pm 0.12	(0.53 \pm 0.11) $\times 10^{-2}$
7299.2 \pm 0.5	7301.1 \pm 0.5	7301.09 \pm 0.17	(0.74 \pm 0.08) $\times 10^{-2}$
8310.5 \pm 0.5	8312.9 \pm 0.5	8312.79 \pm 0.14	(3.3 \pm 0.4) $\times 10^{-2}$
8568.8 \pm 1.0	8571.4 \pm 1.0	8576 \pm 2	(0.43 \pm 0.07) $\times 10^{-2}$
9047.1 \pm 0.7	9050.0 \pm 0.7	9052 \pm 3	(3.1 \pm 0.3) $\times 10^{-2}$

^a Listed in Ref. 1. Accurate values are due to R. C. Greenwood and R. G. Helmer, Nucl. Instrum. Methods 121, 385 (1974).

^b Reference 23.

^c Reference 2. All other intensities are normalized to this value.

areas in a 3-h run and then normalizing by standard methods. Energies for the γ -ray transitions were found by weighting the results from the separate full-energy, one-escape, and two-escape positions and using an energy calibration function based on the peaks present in the spectrum due to the 6129.170 \pm 0.043²² and 7115.15 \pm 0.14-keV²³ γ rays in the decay of ^{16}N . Results for the γ -ray energies and intensities are shown in Table I. By adding the recoil corrections the energies obtained for the ^{15}N excited states are given in column 2 of Table I and compared with previous values as given in the third column.

A special comment is needed on peaks observed in the spectrum at 6322 and 5809 keV. While there was no doubt that the 6322-keV peak corresponded to the ground-state γ -ray transition from the 6323.85-keV level¹ in ^{15}N , the 5809-keV peak was four times too intense to be due to the 6322-keV one-escape peak alone, even though the separation between these peaks was close to 511 keV (actually 513 keV). It was concluded that the 5809-keV line

was caused largely by the random summing of 5298- and 511-keV full-energy-loss pulses. The width of the 5809-keV line was, in fact, almost twice as great as other lines near 6 MeV and this could be explained by summing of the 5298-keV peak with the naturally broadened 511-keV peak. Thus in deriving the energy and relative intensity for the 6322-keV γ ray given in Table I only the full-energy-loss peak was used.

The γ -ray intensities in Table I may be converted into β -ray branches by correcting for the ground-state γ -ray branching intensities as measured most accurately by Phillips, Young, and Marion.²⁴ The β branches are listed in the second column of Table II where the β branches to the ground and 5299-keV levels of ^{15}N are from Ref. 2. For those states above 7 MeV the cascade γ -ray feeding from higher ^{15}N levels is negligible compared with the direct ^{15}C β -ray branching intensity and no further corrections are needed. However, the states at 8313, 8571, and 9050 keV all have γ -ray branches to the 6324-keV level.

TABLE II. β -ray branches in the decay of ^{15}C ($J^\pi = \frac{1}{2}^+$).

State in ^{15}N (keV)	J^π	β -ray branch %		$\log ft$ (present)
		Present	Previous	
0	$\frac{1}{2}^-$	32 \pm 2 ^a	32 \pm 2 ^a	5.99 \pm 0.03
5299	$\frac{1}{2}^+$	68 \pm 2 ^a	68 \pm 2 ^a	4.08 \pm 0.01
6324	$\frac{3}{2}^-$	$\leq 0.4 \times 10^{-2}$		≥ 7.8
7301	$\frac{3}{2}^+$	(0.74 \pm 0.08) $\times 10^{-2}$	(0.8 \pm 0.2) $\times 10^{-2}$ ^b	6.89 \pm 0.05
8313	$\frac{1}{2}^+$	(4.1 \pm 0.5) $\times 10^{-2}$	(5.0 \pm 0.6) $\times 10^{-2}$ ^b	5.18 \pm 0.05
8571	$\frac{3}{2}^+$	(1.3 \pm 0.2) $\times 10^{-2}$	$< 2.8 \times 10^{-2}$ ^b	5.34 \pm 0.07
9050	$\frac{1}{2}^+$	(3.4 \pm 0.3) $\times 10^{-2}$	(3.5 \pm 0.5) $\times 10^{-2}$ ^b	4.05 \pm 0.04

^a Reference 2.

^b Reference 5.

The expected strength of the 6324-keV ground-state transition due to the cascade feeding from these three higher states can be calculated from the β -ray branches in Table II together with the γ -ray branching information in Ref. 24. When the various cascades are added the expected intensity of the 6324-keV transition due to them is $(0.33 \pm 0.08) \times 10^{-2}\%$ per decay. Since this differs from the observed intensity $(0.53 \pm 0.11) \times 10^{-2}\%$ by just the sum of the errors, the appearance of this γ ray could therefore be due entirely to cascade feeding. At least there is no definitive evidence for a direct β -ray branch to the 6324-keV level, and one can only place an upper limit of $\leq 0.4 \times 10^{-2}\%$ on the β -ray branching intensity as given in Table II.

B. ^{15}C Half-life

The half-life of ^{15}C was determined by bombarding the target for 1.5 sec, transferring the rabbit in 0.7 sec, and then multiscaling the β rays at an advance rate of 0.2 sec per channel for 256 channels (51.2 sec or 21 half-lives). Fifteen runs were made using β -ray biases between 1.5 and 3.75 MeV, and the various runs had 20 000 to 40 000 counts in the first channel. Two-component fits starting in the first or 14th channel were made using a computer program and assuming $T_2 = \infty$ for the long-lived background. In none of the runs was the background more than 10^{-4} times as intense as the counting rate in the first channel. At the counting rates used, dead-time effects in the early channels were estimated to be negligible. This was confirmed by the consistency of results from analyses beginning in the first and 14th channels.

In spite of the very clean aspect of the resulting decay curves and the acceptable χ^2 values of the computer fits, there was concern about the effect of the small ^{16}N contaminant activity which was known to be present and which has a half-life of 7.13 sec.²⁵ The relative strength of the ^{16}N component was calculated from the γ -ray data discussed in the preceding section by determining the area under the weak 6129(0) peak, finding its intensity relative to the 5299(0) peak of ^{15}C , and correcting for peak efficiency versus γ -ray energy. The corresponding ^{15}C and ^{16}N β -ray branches are both 68%. From the ratio of $^{16}\text{N}/^{15}\text{C}$ β -ray activities, as determined for the irradiate-count cycle used for the γ -ray measurements, it was found that the relative fraction of ^{16}N in the first channel, for the irradiate-count cycle used in multiscaling the β rays, was 0.030% of the total rate in the first channel.

While this small amount of ^{16}N contamination might have been expected to have a negligible ef-

fect on the result for the ^{15}C half-life, it was felt that the actual effect should be evaluated by using computer techniques. This was done in two ways in the first of which exponential decay curves with $T_{1/2}$ values of 2.46 sec and 7.13 sec were constructed so as to simulate the multiscale operation at 0.2 sec per channel for 256 channels. The total decay curve consisted of a 2.46-sec component with 20 000 counts in the first channel, a constant background of 3 counts per channel, and a variable strength of the ^{16}N exponential. These curves were analyzed with the two-component computer program just as the experimental half-life data had been treated. The percentage increase in the derived ^{15}C half-life is plotted in Fig. 2 (solid points) versus the percentage admixture of the ^{16}N exponential in the first channel, where the two curves are for analyses beginning in the first and 14th channel. The error bars, given by the computer and shown at an admixture of 0.2% of ^{16}N , actually have about the same value for all other points on each respective curve. In a second test one of the experimental runs was used that had 22 000 counts in the first channel and $\chi^2 = 0.961$. Various amounts of a constructed ^{16}N component were added and the total decay curve was analyzed by a two-component fit. Results are shown by the crosses in Fig. 2 which agree very well with results obtained in the first set of analyses described above.

Some general conclusions may be drawn from

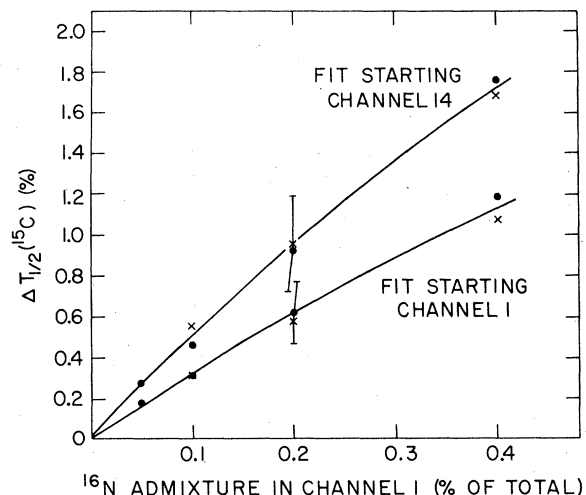


FIG. 2. Change in the apparent half-life of ^{15}C in %, obtained in a two-component fit with $T_2 = \infty$, versus an admixture of ^{16}N activity in % of yield in the first time channel. Curves are results for fits starting in the 1st and 14th channels where the multiscale advance rate was 0.2 sec per channel. Solid points, crosses, and error bars are explained in the text.

the data shown in Fig. 2. In view of the error bars displayed it would appear to be very difficult to determine that a component of ^{16}N was present at the level of 0.1% admixture or less, just on the basis of differences of results obtained by starting the half-life analysis at channel 1 or 14. Starting the analysis in even later channels would not improve matters because the fitting error becomes increasingly larger. In the second set of analyses the χ^2 values were slightly larger than with no ^{16}N added, but even in the worst case the χ^2 was 1.008 which normally would not lead one to suspect that a contaminant activity was present. Another way of detecting the presence of a contaminant is to see if the result depends on the β -ray bias used. However, in the present case the β -ray energies and branching ratios are so close to each other that no bias effect can be expected.

There has been a continuing effort at various laboratories to measure half-lives with accuracies at the level of $\pm 0.1\%$ or better. As Fig. 2 shows, a systematic error of as much as 0.2% in the half-life of ^{15}C could result from an unsuspected ^{16}N contaminant, if one were to depend on the usual tests of varying the β -ray bias and starting the fitting analysis at different channels. If it were not for γ -ray data taken with very good statistical accuracy, the ^{16}N component would go undetected and a correction could not be made. It may be surmised that in any given half-life measurement the quoting of an error of better than $\pm 0.2\%$ carries with it the assumption that no interfering β -emitting contaminants are present in the source.

In the present work corrections can be made using the values on the two curves in Fig. 2 corresponding to an initial ^{16}N admixture of 0.03%. Based on the data of all 15 runs, analyzed as described above, and corrected for the ^{16}N admixture, the final adopted half-life of ^{15}C is 2.449 ± 0.005 sec. This agrees within errors with the previous result of 2.46 ± 0.01 sec obtained²⁶ at this laboratory using the $^{14}\text{C}(d,p)^{15}\text{C}$ reaction. Examination of the old γ -ray data taken⁵ under conditions similar to the half-life measurements²⁶ shows that weak lines were present due to a ^{16}N contaminant. While it would be difficult to apply a meaningful correction to the old half-life data, it is clear from the above analysis that the 2.46-sec value almost certainly would have been reduced slightly, had the necessity for a correction due to the ^{16}N been realized.

This new value for the ^{15}C half-life has been used together with the β -ray branching ratios given in the third column of Table II to derive the experimental $\log ft$ values given in the fifth column of the table. β -decay energies were obtained from

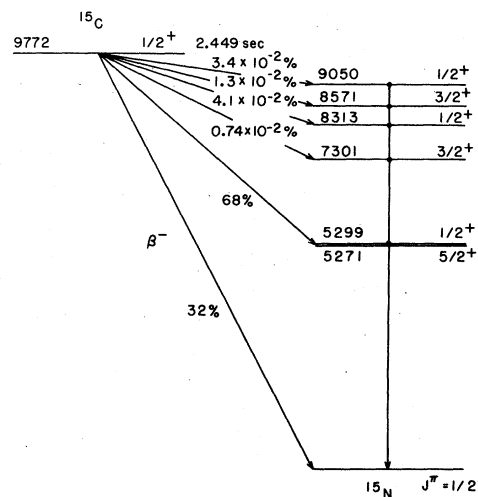


FIG. 3. Decay scheme of ^{15}C . β -ray branches to the ground and 5299-keV states are from Ref. 2. All other branches and the half-life are from the present work.

the most recent compilation¹ and a desk calculator program²⁷ was used to compute the f values. The proposed decay scheme for ^{15}C is shown in Fig. 3.

IV. THEORETICAL RESULTS AND DISCUSSION

A. Preamble

It is convenient to discuss the low-lying positive-parity states of ^{15}N within the framework of the weak coupling model.^{12,28} The most important components of the lowest 1p-2h states arise from the coupling of an $s_{1/2}$ or $d_{5/2}$ nucleon to the 1^+ , $T=0$ ground state and the 0^+ , $T=1$ level at 2.31 MeV of the $A=14$ system. The fact that the $\frac{5}{2}_1^+$ level at 5.27 MeV and the $\frac{1}{2}_1^+$ level at 5.30 MeV are seen strongly in stripping reactions^{1,29} on a ^{14}C target and that the $\frac{5}{2}_2^+$ level at 7.16 MeV, $\frac{3}{2}_1^+$ level at 7.30 MeV, $\frac{7}{2}_1^+$ level at 7.57 MeV and $\frac{1}{2}_2^+$ level at 8.31 MeV are seen strongly in stripping reactions^{1,30-32} on a ^{14}N target confirms this picture. Most shell-model calculations give spectroscopic factors in accord with those extracted from the data. The remaining $\frac{3}{2}_2^+$ configuration which can be constructed from 1^+ , $T=0 \times d_{5/2}$ cannot be identified as a major component of the second $\frac{3}{2}_2^+$ level at 8.58 MeV since the $^{14}\text{N}(d,p)^{15}\text{N}$ spectroscopic factor for this level is very small. Rather it probably forms a large component of the $\frac{3}{2}_3^+$ level at 10.07 MeV.^{30,32}

Since the 1^+ , $T=0$ and 0^+ , $T=1$ levels of the core together with the 1^+ , $T=0$ level at 3.95 MeV in ^{14}N play an important role in discussions of the ^{15}N positive parity levels, it is worthwhile to examine their wave functions in detail. Within a p -shell model space the LS coupling wave functions, using the Cohen and Kurath (8-16)2BME set of matrix elements,³³ are

$$\begin{aligned}
|1_1^+, T=0\rangle &= -0.959 |(02)L=2S=1\rangle \\
&\quad -0.042 |(02)L=0S=1\rangle \\
&\quad +0.280 |(10)L=1S=0\rangle, \\
|1_2^+, T=0\rangle &= 0.040 |(02)L=2S=1\rangle \\
&\quad +0.959 |(02)L=0S=1\rangle \\
&\quad +0.280 |(10)L=1S=0\rangle \\
|0_1^+, T=1\rangle &= 0.847 |(02)L=0S=0\rangle \\
&\quad +0.532 |(10)L=1S=1\rangle.
\end{aligned}$$

Although they are redundant here we have included the SU(3) quantum numbers in labeling the basis states. In a jj coupling basis the wave functions are

$$\begin{aligned}
|1_1^+, T=0\rangle &= 0.950 p_{1/2}^2 p_{3/2}^8 \\
&\quad -0.313 p_{1/2}^3 p_{3/2}^7 \\
&\quad +0.027 p_{1/2}^4 p_{3/2}^6, \\
|1_2^+, T=0\rangle &= 0.282 p_{1/2}^2 p_{3/2}^8 \\
&\quad +0.888 p_{1/2}^3 p_{3/2}^7 \\
&\quad +0.364 p_{1/2}^4 p_{3/2}^6, \\
|0_1^+, T=1\rangle &= 0.923 p_{1/2}^2 p_{3/2}^8 \\
&\quad +0.384 p_{1/2}^4 p_{3/2}^6.
\end{aligned}$$

The β decay of ^{15}C , which proceeds from a rather pure $0_1^+, T=0 \times s_{1/2}$ configuration, will therefore be very slow to $1_1^+, T=0 \times s_{1/2}$ configurations (cf. the ^{14}C β decay). Thus the transitions to the $\frac{3}{2}_1^+$ and $\frac{1}{2}_2^+$ level are expected to be slow as indeed they are (see Table II). On the other hand, transitions to states of the form $0_1^+, T=1 \times s_{1/2}$ or $1_2^+, T=0 \times s_{1/2}$ will be fast. For a pure weak coupling ^{15}C ground state the $\log ft$ values for transitions to the $J=\frac{1}{2}, T=\frac{1}{2}$ weak coupling states with these configurations are 3.3 and 3.4, respectively. Now, however, there is another point to be considered and to discuss it we take the $A=14$ wave functions to be pure LS wave functions corresponding to the dominant component in each state. The ^{15}C ground state then has pure $[4^3 21]$ spatial symmetry and $L=0$, while the $0_1^+, T=1 \times s_{1/2}$ and $1_2^+, T=0 \times s_{1/2}$ configurations with $T=\frac{1}{2}$ are equal admixtures of $[4^3 3]$ and $[4^3 21]$ spatial symmetry with $L=0$. The effective particle-hole interaction mixes the two weak coupling configurations in such a way as to make the $[4^3 3]$ symmetry dominant in the lower state. Since the Gamow-Teller transition can proceed only to the $[4^3 21]$ component, the transition to the lower state can be slowed down considerably and vanishes in the limit of good spatial symmetry. Halbert and French,⁶ Zhusupov, Karapetyan, and Eramzhyan,⁷ and Hsieh and Horie⁸ all used a Rosenfeld interaction which has a

strong space exchange component for their particle-hole force. This leads to too pure $[4^3 3]$ symmetry in the $\frac{1}{2}_1^+$ wave function and a $\log ft$ of ~ 4.8 to be compared with the experimental value of 4.08. We note that any substantial 3p-4h component in the $\frac{1}{2}_1^+$ wave function will slow the transition down even more. Richter and de Kock,⁹ on the other hand, calculate $\log ft$ values in the range 3.5-3.6 for this transition. The reason is clearly the omission of the $p_{3/2}$ orbit from their calculation which makes it impossible to describe the important $1_2^+, T=0$ configuration of the core. Their $\log ft$ values for the other transitions are also in poor agreement with the experimental data. This illustrates the general point that it is important to include both members of a spin-orbit doublet in the shell-model basis when matrix elements of spin-dependent operators are required.

For a discussion of the β transitions to the $\frac{3}{2}_2^+$ level at 8.57 MeV and the $\frac{1}{2}_3^+$ level at 9.05 MeV, the inclusion of 3p-4h states in the basis must be considered. The arguments for the importance of these configurations in a description of the positive parity states of ^{15}N have been summarized by Lie, Engeland, and Dahll.¹² The $\frac{9}{2}_1^+$ level at 10.69 MeV in ^{15}N is very strongly populated in three particle transfer reactions³⁴ on a ^{12}C target and is therefore thought to have a large ^{12}C g.s. $\times {}^{19}\text{F}(\frac{9}{2}_1^+)$ component. If we assume that the lowest 3p-4h states with $J \leq \frac{5}{2}$ also have major ^{12}C g.s. $\times {}^{19}\text{F}(J_1^+)$ components, then we expect to find $J \leq \frac{5}{2}$ states with large 3p-4h components above ~ 8 MeV in ^{15}N and below the $\frac{9}{2}_1^+$ level at 10.69 MeV. Certainly such states are needed to obtain the correct number of positive-parity levels in this region of excitation energy.

In the case of the $\frac{1}{2}_1^+, T=\frac{1}{2}$ levels, the 3p-4h state just described will have predominantly $L=0$. It will therefore mix very little with the $1_1^+, T=0 \times s_{1/2}$ configuration and thus the $\frac{1}{2}_2^+$ level at 8.31 MeV should retain a rather pure 1p-2h character. The $0_1^+, T=1 \times s_{1/2}$ and $1_2^+, T=0 \times s_{1/2}$ configurations have predominantly $L=0$ and can be expected to mix with the 3p-4h state. If the $\frac{1}{2}_3^+$ level has a large 3p-4h component, it must have acquired an appreciable 1p-2h component (with $[4^3 21]$ symmetry) through mixing to explain the moderately fast β transition with $\log ft=4.05$. We have already noted that the $\frac{3}{2}_2^+$ level at 8.57 MeV is weakly populated in single-particle stripping reactions suggesting that it contains configurations consisting of a particle coupled to excited states of the $A=14$ core and/or 3p-4h configurations. In the absence of an appreciable $1_2^+, T=0 \times s_{1/2}$ component, which is likely since the 3p-4h and other 1p-2h configurations have mainly $L=2$, the β transition to this level should be slow as is indeed

observed.

Our discussion thus far has made use of a few weak coupling configurations to give a broad view of the structure of the low-lying positive parity states of ^{15}N . Other weak coupling basis states are of importance also and in the next section we turn to a shell-model calculation performed in an SU(3) basis. It is not difficult to construct the pure weak coupling wave functions in terms of the SU(3) basis states, and it is therefore straightforward to test the general arguments given in this section. We note that the pure weak coupling basis states do contain spurious center-of-mass components, while the full shell-model wave functions are free of such components.

B. Shell model calculation

Our shell-model calculations are performed in an SU(3) basis. All $1\hbar\omega$ configurations are included, i.e.,

$$\begin{aligned} p^{10} \times sd: & (02) \times (20) - (22) (11) (00) [4^33] [4^321], \\ & (10) \times (20) - (30) (11) [4^33] [4^2331], \\ s^{-1}p^{12}: & (00) [4^33]. \end{aligned}$$

Although our basis states do not have good overall spatial symmetry, we have indicated the possible $[f]$ as well as $(\lambda\mu)$ for each configuration. The most important SU(3) couplings for the $3\hbar\omega$ states are

$$\begin{aligned} p^8 \times sd^2: & (04) \times (60) - (64) (53) (42) (31) (20) \\ & \times (22) - (26) (42) \dots \\ & \times (41) - (45) (53) (42) \dots \\ & (12) \times (60) - (72) (53) (42) \dots \\ & (41) - (53) (42) \dots \\ p^9 sdpf: & (03) \times (20) \times (30) - (53) (42) \dots \end{aligned}$$

Our main calculation includes all states with $S \leq \frac{3}{2}$ and $(\lambda\mu) = (64) (26) (45) (72) (53)$. The restriction on S helps to limit the size of the basis, but for given $(\lambda\mu)$ does allow all states from the two most important spatial symmetries, $[4^33]$ and $[4^321]$. We have also included the (42) representation in some test calculations; in this case we also include the $s^{-1}p^{10}sd^2$ configuration but omit the $p^{10}sdg$ configuration, a procedure which introduces a very small amount of spuriousity into the wave functions.

The interactions used are the Cohen and Kurath (8-16)2BME interaction³³ in the p shell, the Kuo-Brown interaction³⁵ in the sd shell, the Millener and Kurath particle-hole interaction,³⁶ and the Kuo bare G matrix³⁷ elsewhere. The p and sd shell single-particle energies have the "experi-

mental" values taken from $A=15$ and $A=17$. Since the s^{-1} and pf configurations are of little importance, other than to ensure proper elimination of spurious center-of-mass components from the wave functions, any "reasonable" set of single-particle energies will suffice for the s and pf orbits. Finally all $3\hbar\omega$ configurations have been lowered by 3.4 MeV to compensate for the quite severe truncation of the basis; note that it is not necessary to do this in weak-coupling calculations²⁸ since a large part of the binding energy is taken from experiment.

In Table III we give the energies of the lowest states of each J for $J \leq \frac{5}{2}$ together with some analysis of the wave functions. For ease of comparison with experiment, we have normalized the excitation energy of the $\frac{1}{2}^+$ level to 5.30 MeV; this entails a downward shift of the entire spectrum by 1 MeV. It is clear that the inclusion of 3p-4h states is necessary to get the correct number of states below ~ 12 MeV. Our calculation may best be compared with that of Lie, Engeland, and Dahll (LED).¹² The essential differences are the following:

- (1) LED use the Gillet interaction³⁸—which is central—to calculate the particle-hole matrix elements. Our interaction contains noncentral components and represents a considerable improvement^{36,39} over purely central forces in the description of non-normal parity states in p -shell nuclei.
- (2) The weak-coupling model uses essentially a product basis rather than a coupled basis with respect to SU(3). Our basis states have good SU(3) symmetry which permits an exact elimination of spurious center-of-mass states.
- (3) LED apparently obtain their 3p-4h states too low in energy. They obtain $\frac{5}{2}^+$ and $\frac{9}{2}^+$ states at 7.75 and 9.94 MeV which they identify, we think correctly, with the experimental levels at 9.15 and 10.69. In the case of the $\frac{1}{2}^+$ levels, they obtain an inversion in level ordering (of $\frac{1}{2}_2^+$ and $\frac{1}{2}_3^+$), and the large 3p-4h component in the $\frac{1}{2}_1^+$ wave function makes it difficult to explain the single nucleon transfer data and the $\log ft$ value. We adjust the unperturbed energy of our $3\hbar\omega$ states, but we think the results give better agreement with the data.

We obtain a very small $3\hbar\omega$ admixture of 0.6% in the ^{15}C ground state wave function. Thus in the β decay there will be very little contribution to the Gamow-Teller matrix element from $3\hbar\omega$ admixtures in the $T = \frac{1}{2}$ wave functions. Rather the major effect of these $3\hbar\omega$ admixtures, which can be large for $T = \frac{1}{2}$, is one of dilution. The lowest 3p-4h states with $T = \frac{1}{2}$ are dominated by the (64) representation; e.g., 83% and 75% for the lowest

TABLE III. Excitation energies (in MeV) and wave functions.

J^π, T	n	E_{expt}	E_{calc}	%1p-2h	%3p-4h	2p-1h weak coupling components
$\frac{1}{2}^+, \frac{1}{2}$	1	5.30	5.30 ^a	88.3	10.6	$0.748 0_1^+, 1 \times \frac{1}{2}^+\rangle + 0.407 1_2^+, 0 \times \frac{1}{2}^+\rangle - 0.261 2_1^+, 1 \times \frac{5}{2}^+\rangle - 0.184 1_1^+, 0 \times \frac{3}{2}^+\rangle$
	2	8.31	8.17	98.8	0.9	$-0.965 1_1^+, 0 \times \frac{1}{2}^+\rangle - 0.151 1^+, 1 \times \frac{1}{2}^+\rangle$
	3	9.05	8.77	12.3	87.6	$-0.295 0_1^+, 1 \times \frac{1}{2}^+\rangle$
	4	11.44	11.91	90.0	9.0	$-0.687 1_2^+, 0 \times \frac{1}{2}^+\rangle + 0.416 1^+, 1 \times \frac{1}{2}^+\rangle + 0.213 3^+, 0 \times \frac{5}{2}^+\rangle - 0.266 0_2^+, 1 \times \frac{1}{2}^+\rangle$
$\frac{3}{2}^+, \frac{1}{2}$	1	7.30	6.30	93.2	6.8	$0.821 1_1^+, 0 \times \frac{1}{2}^+\rangle - 0.274 1_2^+, 0 \times \frac{5}{2}^+\rangle + 0.294 2_1^+, 1 \times \frac{1}{2}^+\rangle + 0.196 2_1^+, 1 \times \frac{5}{2}^+\rangle$
	2	8.57	8.58	66.7	33.3	$-0.452 1_2^+, 0 \times \frac{5}{2}^+\rangle - 0.426 1_1^+, 0 \times \frac{5}{2}^+\rangle + 0.274 0_1^+, 1 \times \frac{3}{2}^+\rangle + 0.228 1_1^+, 0 \times \frac{3}{2}^+\rangle$
	3	10.07	10.30	89.5	10.5	$-0.805 1_1^+, 0 \times \frac{5}{2}^+\rangle - 0.358 1_1^+, 0 \times \frac{3}{2}^+\rangle + 0.210 1_2^+, 0 \times \frac{3}{2}^+\rangle$
	4	10.80	10.90	48.8	51.2	$-0.427 1_2^+, 0 \times \frac{5}{2}^+\rangle + 0.312 0^+, 1 \times \frac{3}{2}^+\rangle + 0.282 1_1^+, 0 \times \frac{3}{2}^+\rangle + 0.216 1_2^+, 0 \times \frac{1}{2}^+\rangle$
	5	11.78	11.75	35.7	64.3	$0.480 1_2^+, 0 \times \frac{1}{2}^+\rangle$
$\frac{5}{2}^+, \frac{1}{2}$	1	5.27	5.48	95.7	4.3	$0.776 0_1^+, 1 \times \frac{5}{2}^+\rangle - 0.325 1_1^+, 0 \times \frac{5}{2}^+\rangle - 0.238 1_2^+, 0 \times \frac{5}{2}^+\rangle - 0.232 1_2^+, 0 \times \frac{3}{2}^+\rangle$ $+ 0.215 1_1^+, 1 \times \frac{3}{2}^+\rangle + 0.200 1_1^+, 1 \times \frac{5}{2}^+\rangle$
	2	7.15	7.41	87.5	12.5	$0.795 1_1^+, 0 \times \frac{5}{2}^+\rangle - 0.307 1_2^+, 0 \times \frac{5}{2}^+\rangle + 0.241 0_1^+, 1 \times \frac{5}{2}^+\rangle$
	3	9.15	9.23	14.3	85.7	$-0.233 1_1^+, 0 \times \frac{5}{2}^+\rangle - 0.261 0_1^+, 1 \times \frac{5}{2}^+\rangle$
	4	10.53	10.76	37.1	62.9	$0.328 2_1^+, 1 \times \frac{1}{2}^+\rangle + 0.263 2^+, 0 \times \frac{1}{2}^+\rangle + 0.222 1_1^+, 0 \times \frac{3}{2}^+\rangle + 0.202 2_1^+, 1 \times \frac{5}{2}^+\rangle$
$\frac{1}{2}^+, \frac{3}{2}$	1	11.62	12.08	99.4	0.6	$0.984 0_1^+, 1 \times \frac{1}{2}^+\rangle - 0.146 2_1^+, 1 \times \frac{5}{2}^+\rangle$

^a Normalized.

$3\hbar\omega$ states with $J = \frac{1}{2}$ and $J = \frac{3}{2}$, respectively (and similarly for other J values). The (72), (53), (45), and (26) representations make decreasing contributions to the wave functions ranging, for $J = \frac{1}{2}$, from $\sim 8\%$ down to $\sim 2\%$. The (42) configurations, when included for $J = \frac{1}{2}$, contributed less than 3% to the wave function (still less for high J values), and we expect that other omitted configurations will be even less important. For comparison a pure weak coupling $^{12}\text{C}(0_1^+) \times ^{19}\text{F}(\frac{1}{2}_1^+)$ wave function would contain rather less (64) ($\sim 55\%$) and much more (42) (some of which would be spurious), but would still have a large overlap with our lowest $3\hbar\omega$ $\frac{1}{2}^+$, $T = \frac{1}{2}$ state.

C. ^{15}C β Decay

The $\log ft$ values calculated from the wave functions presented in Table III are given in Table V. However, before discussing these results we first compare in Table IV the results of our calculations restricted to a $1\hbar\omega$ space with those that have been published previously. The first three all use the Rosenfeld exchange mixture for their central particle-hole interaction. However, they differ in their treatment of the core, so we expect some differences in the calculated $\log ft$ values. The results presented in Table IV suggest that in a $1\hbar\omega$ calculation only the $\log ft$ values for $\frac{1}{2}_1^+$, $\frac{1}{2}_2^+$,

TABLE IV. $1\hbar\omega$ calculations for the β decay of ^{15}C .

	E	$\log ft^a$	E	$\log ft^b$	E	$\log ft^c$	E	$\log ft^d$	E	$\log ft^e$	E	Expt ^e $\log ft$
$\frac{1}{2}_1^+$	5.30 ^f	4.80	5.30 ^f	4.76	5.30 ^f	4.7	5.30 ^f	3.52	5.30 ^f	4.12	5.30	4.08 ± 0.01
$\frac{1}{2}_2^+$	8.5	4.51	8.54	4.66	7.34	5.6	7.6	3.74	7.83	4.89	8.31	5.18 ± 0.05
$\frac{1}{2}_3^+$	11.5		11.39	4.02		4.1			11.89	3.46	11.44	
$\frac{3}{2}_1^+$	6.5	6.49	6.34	4.83	6.22	6.1	6.8	4.01	6.29	5.77	7.30	6.89 ± 0.05
$\frac{3}{2}_2^+$	7.7		7.93	5.34	8.71	4.7	7.9	∞	9.09	4.76	8.57	5.34 ± 0.07

^a References 6, 2.^b Reference 7.^c Reference 8.^d Reference 9.^e Present.^f Normalized.

and $\frac{3}{2}_1^+$ may be legitimately compared with experiment. The high energy calculated for $\frac{1}{2}_3^+$ in the $1\hbar\omega$ calculations also makes it unlikely that this state can be identified with the 9.05-MeV level. For the $\frac{3}{2}_2^+$ level the situation is less clear cut. Both LED's calculations¹² and the present one obtain considerable mixing between $1\hbar\omega$ and $3\hbar\omega$ configurations. Also both calculations concentrate the $(1_1^+, 0 \times d)_{\frac{3}{2}}^+$ strength in the third model state and identify this state with the 10.07-MeV level which is strongly populated in the $^{14}\text{N}(d, p)^{15}\text{N}$ reaction.^{30,32} The fourth set of results in Table IV emphasizes the inadequacy of omitting the $p_{3/2}$ orbit from the calculation. Finally, our results show that an improvement results, particularly for the $\frac{1}{2}_1^+$ level, from using a particle-hole interaction with a weaker space exchange component than the Rosenfeld interaction. The MK interaction³⁶ has $M=0.65$ to be compared with $M=0.93$ for the Rosenfeld interaction. The particle-hole interaction should perhaps be weakened or the exchange mixture adjusted to further lessen the influence of the $1_2^+, 0 \times s_{1/2}$ configuration in the $\frac{1}{2}_1^+$ wavefunction.

There will clearly be large GT matrix elements to states of predominantly $[4^321]$ symmetry which are too high in energy to be reached in the ^{15}C β decay. In our $1\hbar\omega$ calculation some of these (up to $E_x = 15$ MeV) are, in the notation $J_n^*(E, \log ft)$; $\frac{3}{2}_3^+(10.06, 4.75)$, $\frac{1}{2}_3^+(11.89, 3.46)$, $\frac{3}{2}_4^+(11.89, 3.28)$, $\frac{3}{2}_5^+(13.93, 4.31)$, $\frac{3}{2}_6^+(14.19, 4.54)$, $\frac{1}{2}_4^+(14.64, 3.98)$, $\frac{3}{2}_7^+(14.68, 4.08)$, and $\frac{1}{2}_5^+(14.99, 3.41)$. It is worth noting the $\log ft$ values for transitions between pure weak coupling states, i.e., with $[0_1^+, 1 \times \frac{1}{2}^+] T = \frac{3}{2}, J = \frac{1}{2}$ as initial state and an $s_{1/2}$ particle coupled to any of the first three states of the $A=14$ core as final state. In the notation $(J_n, J_f, \log ft)$, where J_n refers to the core, they are $(1_1, \frac{1}{2}, 5.89)$, $(0_1, \frac{1}{2}, 3.31)$, $(1_2, \frac{1}{2}, 3.40)$, $(1_1, \frac{3}{2}, 5.59)$, and $(1_2, \frac{3}{2}, 3.10)$. The first and fourth of these are trivially related to the $\log ft$ value for the ^{14}C β decay

$$\log ft(^{15}\text{C}) = \log ft(^{14}\text{C}) + \log \left(\frac{6}{2J_f + 1} \right).$$

The observed $\log ft$ value for ^{14}C decay is 9.02 which corresponds to essentially complete cancellation in the Gamow-Teller matrix element. The Cohen and Jurath (8-16)2BME interaction³³ gives a $\log ft(^{14}\text{C}) = 5.42$ and complete cancellation can be achieved⁴⁰ by slightly reducing the spin-orbit splitting between the $p_{3/2}$ and $p_{1/2}$ orbits (Fig. 3 of Ref. 40). In the final column of Table V we give $\log ft$ values obtained in the full calculation for a value of the p -shell spin-orbit splitting close to the cancellation point for the ^{14}C matrix element. $\log ft(\frac{1}{2}_2^+)$ has already passed

TABLE V. $\log ft$ values from present calculations: Case A $1\hbar\omega$ only, case B full calculation, case C reduced p -shell spin orbit splitting.

E_{exc} (MeV)	J_n^π	Expt	A	B	C
5.30	$\frac{1}{2}_1^+$	4.08	4.12	4.24	4.34
8.31	$\frac{1}{2}_2^+$	5.18	4.89	4.88	5.37
9.05	$\frac{1}{2}_3^+$	4.05		4.52	4.52
7.30	$\frac{3}{2}_1^+$	6.89	5.77	5.52	5.94
8.57	$\frac{3}{2}_2^+$	5.34	4.77	4.82	4.82

from below the experimental value to above it (Table V), while $\log ft(\frac{3}{2}_1^+)$ has also increased but not enough to reproduce the data.

To summarize, then, the situation for the $\frac{1}{2}_1^+$, $\frac{3}{2}_1^+$, and $\frac{1}{2}_2^+$ levels is that the calculation describes rather well the β decay and single nucleon transfer data. A larger 3p-4h component in the $\frac{1}{2}_1^+$ wave function could be tolerated, but to have dominant 3p-4h component would be in conflict with the single nucleon transfer data. The 1p-2h components in the $\frac{1}{2}_3^+$ wave function have predominantly $T_h=1$. The calculated $^{14}\text{C}(d, n)^{15}\text{N}(\frac{3}{2}_3^+)$ spectroscopic factor is 0.09. Were we to scale the intensity of $1\hbar\omega$ components in the wave function to reproduce the $\log ft$ value, the spectroscopic factor would be 0.26 to be compared with the observed value²⁹ of 0.30. Thus a way must be found to enhance the $1\hbar\omega$ component in our $\frac{1}{2}_3^+$ wave function. The $\frac{3}{2}_2^+$ level is the least understood of the five discussed here. We obtain an appreciable 3p-4h component in the $\frac{3}{2}_2^+$ wave function. Even so the predicted $^{14}\text{N}(d, p)^{15}\text{N}(\frac{3}{2}_2^+)$ spectroscopic factor is too large by a factor of 2,³⁰ and the predicted β transition is too fast by a factor of 3. We have not studied the first-forbidden nonunique β transition to the ^{15}N ground state in view of the comprehensive treatment by Towner and Hardy.¹⁰

Although our calculations represent an improvement over previous studies of the Gamow-Teller transitions from the β decay of ^{15}C , the agreement that we obtain with experiment is still not satisfactory. Further studies must concentrate on the way in which the $1\hbar\omega$ configurations mix with higher configurations and attempt to explain the radiative decays to and from, and the Coulomb energy shifts of, the levels of interest in the β decay of ^{15}C .

We would like to thank E. K. Warburton for helpful comments. This research was supported by the Division of Basic Energy Sciences, Department of Energy under Contract No. EY-76-C-02-0016.

- ¹F. Ajzenberg-Selove, Nucl. Phys. A268, 1 (1976).
- ²D. E. Alburger, A. Gallmann, and D. H. Wilkinson, Phys. Rev. 116, 939 (1959).
- ³D. E. Alburger, C. Chasman, K. W. Jones, and R. A. Ristinen, Phys. Rev. 136, B913 (1964).
- ⁴D. E. Alburger and K. W. Jones, Phys. Rev. 149, 743 (1966).
- ⁵A. Gallmann, F. Jundt, E. Aslanides, and D. E. Alburger, Phys. Rev. 179, 921 (1969).
- ⁶E. C. Halbert and J. B. French, Phys. Rev. 105, 1563 (1957).
- ⁷M. A. Zhusupov, V. V. Karapetyan, and R. A. Eramzhyan, Izv. Acad. Nauk. SSSR 32, 334 (1968) [Bull. Acad. Sci. USSR, Phys. Ser. 32, 305 (1968)].
- ⁸S. T. Hsieh and H. Horie, Nucl. Phys. A151, 243 (1970).
- ⁹W. A. Richter and P. R. de Kock, Z. Phys. A282, 207 (1977).
- ¹⁰I. S. Towner and J. C. Hardy, Nucl. Phys. A179, 489 (1972).
- ¹¹S. T. Hsieh, K. T. Knöpfle, G. Mairle, and G. J. Wagner, Nucl. Phys. A243, 380 (1975).
- ¹²S. Lie, T. Engeland, and G. Dahl, Nucl. Phys. A156, 449 (1970).
- ¹³I. Unna and I. Talmi, Phys. Rev. 112, 452 (1958).
- ¹⁴A. P. Shukla and G. E. Brown, Nucl. Phys. A112, 296 (1968).
- ¹⁵A. P. Zuker, B. Buck, and J. B. McGrory, Phys. Rev. Lett. 21, 39 (1968); Brookhaven National Laboratory informal Report No. PD-99, BNL 14085.
- ¹⁶B. S. Reehal and B. H. Wildenthal, Part. Nucl. 6, 137 (1973).
- ¹⁷R. Saayman and P. R. de Kock, Z. Phys. 266, 83 (1974).
- ¹⁸J. B. McGrory and B. H. Wildenthal, Phys. Lett. 60B, 5 (1975).
- ¹⁹G. E. Schwender, D. R. Goosman, and K. W. Jones, Rev. Sci. Instrum. 43, 832, (1972).
- ²⁰J. C. Hardy and D. E. Alburger, Phys. Lett. 42B, 341 (1972).
- ²¹W. R. Kane and M. A. Mariscotti, Nucl. Instrum. Methods 56, 189 (1967).
- ²²E. B. Spera, Phys. Rev. C 12, 1003 (1975).
- ²³D. E. Alburger, Nucl. Instrum. Methods 136, 323 (1976).
- ²⁴G. W. Phillips, F. C. Young, and J. B. Marion, Phys. Rev. 159, 891 (1967).
- ²⁵F. Ajzenberg-Selove, Nucl. Phys. A166, 1 (1971).
- ²⁶D. E. Alburger and G. A. P. Engelbertink, Phys. Rev. C 2, 1594 (1970).
- ²⁷D. H. Wilkinson and B. E. F. Macefield, Nucl. Phys. A232, 58 (1974).
- ²⁸P. J. Ellis and T. Engeland, Nucl. Phys. A144, 161 (1970).
- ²⁹J. Bommer, M. Ekpo, H. Fuchs, K. Grabisch, and H. Kluge, Nucl. Phys. A251, 246 (1975).
- ³⁰G. W. Phillips and W. W. Jacobs, Phys. Rev. 184, 1052 (1969).
- ³¹J. Bommer, H. Fuchs, K. Grabisch, U. Janetski, and G. Röscher, Nucl. Phys. A172, 618 (1971).
- ³²A. Amokrane, M. Allab, H. Beaumevielle, B. Faid, O. Bersillon, B. Chambon, D. Drain, and J. L. Vidal, Phys. Rev. C 6, 1934 (1972).
- ³³S. Cohen and D. Kurath, Nucl. Phys. 73, 1 (1965).
- ³⁴L. H. Harwood, K. W. Kemper, J. D. Fox, and A. H. Lumpkin, Phys. Rev. C 18, 2145 (1978) and references contained therein.
- ³⁵T. T. S. Kuo and G. E. Brown, Nucl. Phys. 85, 40 (1966).
- ³⁶D. J. Millener and D. Kurath, Nucl. Phys. A255, 315 (1975).
- ³⁷T. T. S. Kuo, Nucl. Phys. A103, 71 (1967).
- ³⁸V. Gillet, Nucl. Phys. 51, 410 (1964).
- ³⁹H. U. Jäger and M. Kirchbach, Nucl. Phys. A291, 52 (1977).
- ⁴⁰H. J. Rose, O. Häusser, and E. K. Warburton, Rev. Mod. Phys. 40, 591 (1968).